



Asymmetrical splitting in the spectrum of stochastic radiation scattered by non-Hermitian materials having \mathcal{PT} symmetry

M. A. Pinto * and P. A. Brandão †*Universidade Federal de Alagoas, Instituto de Física, 57072-900, Brazil*

(Received 4 February 2020; accepted 17 April 2020; published 6 May 2020)

The scattering of partially coherent radiation by a localized continuous material having parity-time (\mathcal{PT}) symmetry is considered under the formalism of classical coherence theory and the assumption that the Born approximation is valid. Our results suggest that the correlation-induced spectral changes are strongly dependent upon the gain and loss properties of the material. In particular, the center frequency of the scattered radiation undergoes a discontinuity as a function of the non-Hermitian parameter characterizing the physical properties of the material. The physical reason behind this abrupt behavior is that the \mathcal{PT} symmetry induces the creation of two asymmetrical frequency bands inside the original Hermitian spectrum. We describe how this splitting occurs and offer possibilities to dynamically characterize the scattered spectrum.

DOI: [10.1103/PhysRevA.101.053817](https://doi.org/10.1103/PhysRevA.101.053817)

I. INTRODUCTION

The temporal and spatial behavior of a classical optical wave field generated by a physical source (or induced by scattering) is utterly unpredictable. It cannot be described by using deterministic field functions if one is really concerned with the true dynamics involved in the propagation process. Important classical dynamical electromagnetic quantities measured in the laboratory, such as the intensity and the spectrum of light, are ultimately dependent upon the statistical behavior of the wave field [1–4]. Also, the appearance of an interference pattern, whether in a space or frequency domain, represents a direct manifestation of the statistical correlations that exist between distinct spacetime points in the optical wave field. In fact, these correlations can generate interesting observable effects such as dramatic changes in the optical spectrum of light when propagated even in free space [5–8]. The physical reason behind this is that the correlation between points in a wave field is a dynamical quantity evolving under two coupled wave equations and possessing, therefore, a dynamics of its own [3]. Correlation-induced spectral changes are also observed in linear scattering systems when the incident radiation is, in general, partially coherent and the material under which the incident field acts is assumed to be deterministic or random. In this case, the spectrum in the far zone will, in general, differ from the source spectrum [9–12]. In such scattering scenarios with partially coherent radiation, the medium is generally assumed to be linear, real, and isotropic. However, with the recent advances of non-Hermitian photonics, one is now able to consider suitable engineered materials, having gain and loss properties, and their influence on the classical coherence properties of the scattered wave field. This approach to scattering problems is the main motivation behind the present paper.

The research field of optics and photonics has received an enormous boost in recent years due to the newly defined concept of parity-time (\mathcal{PT}) symmetry [13–15]. It has been recognized since 1998 by Bender and Boettcher that Hamiltonians that are invariant under the \mathcal{PT} -symmetry condition can have real eigenvalues [16–20]. This opens the possibility to extend real, Hermitian systems into the complex domain, thus generalizing Hermitian quantum mechanics, through a new definition of the inner product of the Hilbert space [21]. It should be remarked, however, that the requirement of \mathcal{PT} symmetry is neither a necessary nor a sufficient condition for the reality of the spectrum [22–24]. To give a specific example, if one looks for the discrete spectrum of the Hamiltonian $H = p^2 - ix$, where p is the momentum and x are the position operators, one finds that its eigenvalues are complex even though this Hamiltonian has \mathcal{PT} symmetry. The reason for the appearance of complex eigenvalues despite the obvious \mathcal{PT} symmetry of the Hamiltonian is that H and \mathcal{PT} do not share the same set of eigenvectors because \mathcal{PT} is an antilinear operator. When this is the case, we say that H has a broken \mathcal{PT} symmetry. On the other hand, the Hamiltonian $H = p^2 + ix^3$ has a discrete spectrum consisting of real and positive numbers. In this case, H has an unbroken \mathcal{PT} symmetry and it shares the same eigenvectors with the \mathcal{PT} operator. Usually, the Hamiltonian H is dependent upon a free parameter β such that when $\beta < \beta_c$ ($\beta > \beta_c$), all eigenvalues are real (complex), where β_c is called the symmetry-breaking point. Indeed, the two Hamiltonians given above are special cases ($\beta = 1$ and $\beta = 3$, respectively) of the class $H_\beta = p^2 - (ix)^\beta$ [16]. The symmetry-breaking point (also called exceptional point) for this class is $\beta_c = 2$, represented by the simple harmonic oscillator [16,25].

Due to the analogy between the paraxial wave equation of optics (in inhomogeneous media) and the time-dependent Schrödinger equation of nonrelativistic quantum mechanics, it became possible to map the time-independent potential function $V(\mathbf{r})$ of quantum theory to the index of refraction

*marcel.pinto@fis.ufal.br

†paulo.brandao@fis.ufal.br

$n(\mathbf{r})$ of an inhomogeneous material [15]. The invariance of the refractive index under the \mathcal{PT} symmetry restricts the class of possible non-Hermitian materials having \mathcal{PT} -symmetric characteristics. The invariance $(\mathcal{PT})^{-1}n(\mathbf{r})\mathcal{PT} = n(\mathbf{r})$ implies that $n^*(-\mathbf{r}) = n(\mathbf{r})$, and if we write $n(\mathbf{r}) = n_R(\mathbf{r}) + in_I(\mathbf{r})$ with $n_{R,I}(\mathbf{r})$ being real functions, then $n_R(-\mathbf{r}) = n_R(\mathbf{r})$ and $n_I(-\mathbf{r}) = -n_I(\mathbf{r})$ must be satisfied to ensure the \mathcal{PT} -symmetry condition. Since the imaginary part of the refractive index is related to the loss and gain properties of the material, \mathcal{PT} symmetry requires a balance between loss and gain. The concepts of \mathcal{PT} symmetry have found numerous applications in a variety of optical scenarios, including unidirectional invisibility [26], lasing [27], microring lasers [28], four-wave mixing [29], and topological insulators [30], to cite a few. Two published articles have considered the influence of \mathcal{PT} -symmetric materials on the classical coherence properties of scattered wave fields [31,32]. It was suggested that the spectral and cross-spectral densities of the scattered radiation are strongly dependent upon the loss and gain properties of the deterministic material causing the scattering. However, in arriving at these claims, two major assumptions were imposed. In [31], the considered material is infinite (albeit continuous) in extension and [32] assumes a finite (albeit discontinuous) material, consisting of two point (δ -Dirac) scatterers. In this paper, we formulate a more realistic scattering scenario where the material has a finite extension in space and is described by a continuous, non-Hermitian index of refraction having \mathcal{PT} symmetry. Our main objective is to unveil the influence of the non-Hermitian parameter describing the material on the spectrum and the directions of the emitted radiation. In particular, we address the following questions: (1) Under what conditions will the loss and gain properties of the material cause a deviation in the spectrum of the scattered radiation compared to its Hermitian counterpart? (2) How does the non-Hermitian parameter of the material change the directional properties of the scattered radiation? The answers to these questions can be obtained once we calculate the spectral density $S(\mathbf{r}, \omega)$ of the scattered radiation. In Sec. II, we provide a revision of the scattering theory for partially coherent radiation. Section III presents the analytic results for a specific class of \mathcal{PT} -symmetric localized continuous materials; in Sec. IV, we present our main results.

II. SCATTERING THEORY FOR PARTIALLY COHERENT RADIATION

The scattering theory for partially coherent radiation is well documented [3]. Here we revise the most important concepts and fix some notation. The incident radiation field is characterized by the ensemble $\{U^i(\mathbf{r}, \omega) = a(\omega)\exp(ik\hat{\mathbf{s}}_0 \cdot \mathbf{r})\}$, where $\hat{\mathbf{s}}_0$ is a unit vector representing the incident direction, ω is the angular frequency, $a(\omega)$ is a random function of the angular frequency, $k = \omega/c$, and c is the speed of light in free space. The cross-spectral density describing correlations for a particular frequency ω of the incident radiation is $W^i(\mathbf{r}_1, \mathbf{r}_2, \omega) = \langle U^{i*}(\mathbf{r}_1, \omega)U^i(\mathbf{r}_2, \omega) \rangle = S^i(\omega)\exp[ik\hat{\mathbf{s}}_0 \cdot (\mathbf{r}_2 - \mathbf{r}_1)]$, where $S^i(\omega) = W^i(\mathbf{r}, \mathbf{r}, \omega) = \langle |a(\omega)|^2 \rangle$ is the incident spectral density, assumed to be independent of position (notice that the incident radiation is spatially fully coherent). The stochastic

scattered radiation U^s is represented by the ensemble $\{U^s(\mathbf{r}, \omega)\}$ and its corresponding cross-spectral density $W^s(\mathbf{r}_1, \mathbf{r}_2, \omega) = \langle U^{s*}(\mathbf{r}_1, \omega)U^s(\mathbf{r}_2, \omega) \rangle$. Once the relation between incident and scattered cross-spectral densities is found, the spectral density $S(\mathbf{r}, \omega) = W^s(\mathbf{r}, \mathbf{r}, \omega)$ of the scattered radiation can be easily obtained. If we consider the scattered radiation in the far zone, this relation is given by [3]

$$W^s(r\hat{\mathbf{s}}_1, r\hat{\mathbf{s}}_2, \omega) = \frac{S^i(\omega)}{r^2} \tilde{F}^*[k(\hat{\mathbf{s}}_1 - \hat{\mathbf{s}}_0), \omega] \tilde{F}[k(\hat{\mathbf{s}}_2 - \hat{\mathbf{s}}_0), \omega], \quad (1)$$

where $\mathbf{r}_1 = r\hat{\mathbf{s}}_1$, $\mathbf{r}_2 = r\hat{\mathbf{s}}_2$ (with $\hat{\mathbf{s}}_{1,2}$ radial unit vectors) and $\tilde{F}(\mathbf{K}, \omega)$ is the Fourier transform of the ‘‘scattering potential’’ $F(\mathbf{r}, \omega) = (1/4\pi)k^2[n^2(\mathbf{r}, \omega) - 1]$,

$$\tilde{F}(\mathbf{K}, \omega) = \int F(\mathbf{r}, \omega) \exp(-i\mathbf{K} \cdot \mathbf{r}) d^3\mathbf{r}, \quad (2)$$

with $n(\mathbf{r}, \omega)$ being the inhomogeneous index of refraction. In deriving (1), the Born approximation was assumed to be valid. The spectral density $S(\mathbf{r}, \omega)$ is obtained from (1) by performing $\hat{\mathbf{s}}_1 = \hat{\mathbf{s}}_2 = \hat{\mathbf{s}}$:

$$S(r\hat{\mathbf{s}}, \omega) = \frac{S^i(\omega)}{r^2} |\tilde{F}[k(\hat{\mathbf{s}} - \hat{\mathbf{s}}_0), \omega]|^2. \quad (3)$$

Relation (3) shows that the spectral density of the scattered radiation is, in general, different from the spectral density of the incident radiation $S^i(\omega)$. The role of classical coherence on scattering was considered in several different contexts, including deterministic and random media [9,10,33–36]. In the next section, we apply the formalism developed here to a class of materials having \mathcal{PT} symmetry and investigate the role of the gain and loss on the spectral density.

III. SPECTRAL DENSITY OF THE SCATTERED RADIATION

The influence of the gain and loss of a material on the classical correlations has been investigated in two somewhat idealized scattering scenarios [31,32]. Here we attempt to create a more realistic model in order to describe the scattering of partially coherent radiation from a localized and continuous \mathcal{PT} -symmetric material. To this end, let us consider one of the many possible classes of scattering potentials described by

$$F(\mathbf{r}, \omega) = \frac{Ak^2}{(2\pi\sigma^2)^{3/2}} \exp\left(-\frac{r^2}{2\sigma^2}\right) (1 + i\vec{\beta} \cdot \mathbf{r}), \quad (4)$$

which is a complex \mathcal{PT} -symmetric extension [$F^*(-\mathbf{r}, \omega) = F(\mathbf{r}, \omega)$] of the Hermitian material considered in [11]. The real and imaginary parts of the (squared) refractive index are

$$\begin{aligned} \text{Re}[n^2(\mathbf{r}, \omega)] &= \frac{2A}{\sigma^3\sqrt{2\pi}} \exp(-r^2/2\sigma^2) + 1, \\ \text{Im}[n^2(\mathbf{r}, \omega)] &= (\vec{\beta} \cdot \mathbf{r}) \frac{2A}{\sigma^3\sqrt{2\pi}} \exp(-r^2/2\sigma^2). \end{aligned} \quad (5)$$

A plot of the real and imaginary parts of $n^2(\mathbf{r}, \omega)$ in the xy plane is shown in Fig. 1. The real vector $\vec{\beta}$ is the non-Hermitian parameter which controls the gain and loss properties of the material; the real parameter σ is associated with the size of the material and A is a constant (we are assuming that σ and A are frequency independent). When compared

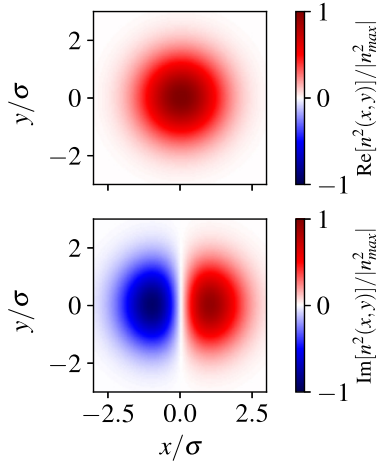


FIG. 1. Normalized real (top) and imaginary (bottom) parts of the (squared) refractive index. Parameters used: $A = 1$, $\lambda = 550$ nm, $\sigma = 3\lambda$, $\vec{\beta} = \beta\hat{x}$, with $\beta = 10^6$ m $^{-3}$.

to previous models [31,32], we see that the proposed system is the only one considering a more realistic scenario with a finite-size, non-Hermitian, and continuous material. Since this represents a more complex scatterer, we expect the formalism to be more involved. However, the Gaussian function chosen to represent the material has a direct, finite, and continuous Fourier transform such that the mathematical analysis can be made without numerical approximations. Certainly there are more classes of continuous functions possessing a Fourier transform as well, and every one should give rise to a different spectral density. A general analysis with arbitrary \mathcal{PT} -symmetric materials is still lacking in the literature.

The Fourier transform of (4) is

$$\tilde{F}(\mathbf{K}, \omega) = Ak^2 \exp\left(-\frac{|\mathbf{K}|^2 \sigma^2}{2}\right) (1 + \sigma^2 \vec{\beta} \cdot \mathbf{K}), \quad (6)$$

and since the spectral density (3) is given in terms of $\mathbf{K} = k(\hat{s} - \hat{s}_0)$, the evaluation of $|\mathbf{K}|^2$ gives

$$|\mathbf{K}|^2 = |k(\hat{s} - \hat{s}_0)|^2 = 4k^2 \sin^2\left(\frac{\theta}{2}\right), \quad (7)$$

where θ is the angle between \hat{s}_0 and \hat{s} . If the material is Hermitian ($\vec{\beta} = 0$), the angle θ would be the only significant spatial quantity characterizing the spectral density. The physical properties of the spectrum would solely depend on the angle between the incident and scattered directions [11]. However, when $\vec{\beta} \neq 0$, the last term in (6) introduces a kind of anisotropic contribution to the spectral density,

$$\vec{\beta} \cdot \mathbf{K} = k(\vec{\beta} \cdot \hat{s} - \vec{\beta} \cdot \hat{s}_0). \quad (8)$$

Clearly, the spectral properties of the scattered radiation in this non-Hermitian context depend not only on the relative orientation between the incident and scattered directions, but also on the relative orientation between the non-Hermitian parameter $\vec{\beta}$ and the incident and scattered directions.

To simplify, consider a particular class of materials described by $\vec{\beta} = \beta\hat{s}_0$, with β constant. Therefore, we are considering the particular situation in which the variation of the imaginary part of the refractive index is in the same direction

as the incident radiation. In this case, relation (8) turns into

$$\vec{\beta} \cdot \mathbf{K} = -2k\beta \sin^2\left(\frac{\theta}{2}\right), \quad (9)$$

and if we assume a Gaussian profile centered at ω_0 for the spectral density of the incident radiation,

$$S^i(\omega) = S_0 \exp\left[-\frac{(\omega - \omega_0)^2}{2\Gamma_0^2}\right], \quad (10)$$

where S_0 is a constant and Γ_0 is the bandwidth, the spectral density of the scattered radiation is finally given by

$$S_\beta(\theta, \omega) = \frac{A^2 S_0}{r^2} \left(\frac{\omega}{c}\right)^4 \times \exp\left[-\frac{(\omega - \omega_0)^2}{2\Gamma_0^2} - 4\left(\frac{\omega}{c}\right)^2 \sigma^2 \sin^2\left(\frac{\theta}{2}\right)\right] \times \left[1 - 2\sigma^2 \beta \left(\frac{\omega}{c}\right) \sin^2\left(\frac{\theta}{2}\right)\right]^2. \quad (11)$$

Equation (11) is the principal result of this paper. We first note that the class of materials described by (4) introduces some dramatic changes on the spectral density of the scattered field, represented by the term inside the brackets. When $\beta = 0$, meaning the class of Hermitian materials, relation (11) reduces to the results previously reported by Lahiri and Wolf where correlation-induced spectral shifts were observed [11]. By making ω , Γ_0 , β , and σ dimensionless through the transformations

$$\omega \rightarrow \frac{\omega}{\omega_0}, \quad \Gamma_0 \rightarrow \frac{\Gamma_0}{\omega_0}, \quad \beta \rightarrow \frac{c}{\omega_0} \beta, \quad \text{and} \quad \sigma \rightarrow \frac{\omega_0}{c} \sigma, \quad (12)$$

and defining the normalized spectral density $S \rightarrow \frac{c^4 r^2 S}{\omega_0^4 A^2 S_0}$, Eq. (11) can be rewritten as

$$S_\beta(\theta, \omega) = \exp\left[-\frac{(\omega - 1)^2}{2\Gamma_0^2} - 4\sigma^2 \omega^2 \sin^2\left(\frac{\theta}{2}\right)\right] \times \left(\omega^2 - 2\beta\sigma^2 \omega^3 \sin^2\left(\frac{\theta}{2}\right)\right)^2. \quad (13)$$

This normalized form of the spectral density is more suitable for the treatment that follows.

IV. NON-HERMITIAN CORRELATION-INDUCED SPECTRAL SHIFTS

A. Frequency analysis

The normalized spectral density of the scattered radiation, represented by Eq. (13), has a very rich and nontrivial structure. To reveal its properties in a more transparent way, we follow Lahiri and Wolf in fixing the scattering angle at $\theta = 24.9^\circ$ and consider Eq. (13) as a function of frequency ω , describing the spectrum profile for each value of the non-Hermitian parameter β . We will later fix the angular frequency ω and observe the spatial distribution of the scattered radiation. One of the many possible useful parameters characterizing a spectral distribution is the center frequency ω_c at which S_β has its maximum value. Since this will depend upon the non-Hermitian parameter β , we are actually interested in

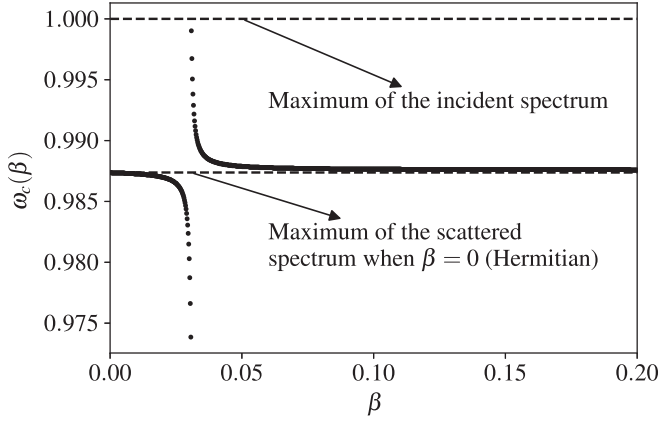


FIG. 2. The dependence of the dimensionless frequency $\omega_c = \omega_c(\beta)$ [such that $S_\beta(\omega_c)$ is a maximum] as a function of the dimensionless parameter β . The two dashed lines indicate the values of ω_c for the incident and scattered spectrum in the Hermitian configuration ($\beta = 0$). The dotted line represents the non-Hermitian situation where a discontinuity around $\beta_c \approx 0.03$ is clearly visible. Parameters used: $\sigma = 6\pi$, $\Gamma_0 = 0.01$, and $\theta = 24.9^\circ$ [in which σ and Γ_0 are the same as [11], but normalized following Eq. (12)].

the functional relation $\omega_c = \omega_c(\beta)$. If one naively plots this dependence directly from Eq. (13), a discontinuity appears, as shown in Fig. 2, at a specific β_c in the interval $\beta \in [0, 0.2]$. The dashed line $\omega_c = 1$ in the figure indicates the center frequency of the incident spectrum, while the bottom dashed line indicates the center frequency where the Hermitian scattered spectral density has a maximum [11]. The first step towards the understanding of this discontinuous behavior is to notice that Eq. (13), viewed as a function of ω , is composed of a product of three functions,

$$g(\omega) = \exp\left[-\frac{(\omega-1)^2}{2\Gamma_0^2}\right], \quad (14)$$

$$h(\omega) = \exp\left(-\frac{\omega^2}{2\Gamma_1^2}\right), \quad (15)$$

$$p_\beta(\omega) = \left(\omega^2 - 2\beta\sigma^2\omega^3 \sin^2\frac{\theta}{2}\right)^2. \quad (16)$$

The non-Hermitian information of the scattering process is contained in the sixth-degree polynomial $p_\beta(\omega)$. The functions $g(\omega)$ and $h(\omega)$ represent Gaussian profiles centered at 1 and 0 and with widths Γ_0 and

$$\Gamma_1 = \frac{1}{[8\sigma^2 \sin^2(\frac{\theta}{2})]^{1/2}}, \quad (17)$$

respectively. The appearance of the discontinuity of the center frequency is due to the fact that the non-Hermitian properties of the material induce the creation of two separate bands inside the original, Hermitian spectrum. The appearance of the two asymmetrical spectral modes displays an interesting dynamics, which we will explain shortly. Figure 3 illustrates the spectral density for three values of the non-Hermitian parameter: $\beta = 0$ (Hermitian case), $\beta = 0.03079$ (below the discontinuity), and $\beta = 0.03054$ (above the discontinuity). The scattered spectrum is strongly modified by the material's gain and loss in such a way that two critical points appear

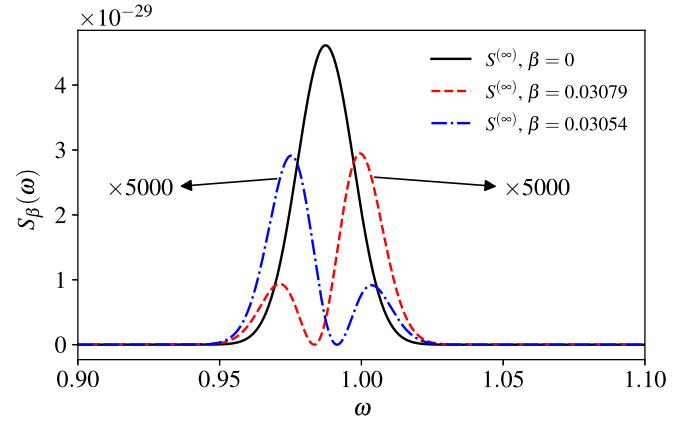


FIG. 3. This figure explains the apparent discontinuous behavior of the center frequency at which S_β is maximum. As the parameter β increases from zero value, the scattered spectrum gets strongly modified and a double frequency band appears in such a way that the global and local maxima switch places as β passes through a critical value. The quantities S_β , ω , and β are dimensionless, as defined in the main text.

inside the bandwidth of the Hermitian spectrum ($\beta = 0$). The dashed red line in Fig. 3 (below the discontinuity) indicates that the spectrum has two critical points (ignoring the minimum at which $S_\beta = 0$). There are global and local maxima that switch places as the parameter β passes through β_c , explaining the discontinuous behavior of ω_c . To perform a quantitative analysis of the switching process, we plot the center frequency of each mode individually as a function of β . The upper part of Fig. 4 displays the behavior of the left mode (smaller in frequency) and the right mode (higher in frequency) as β varies. It is clear that there is a correlation-induced spectral shift caused by the non-Hermitian parameter

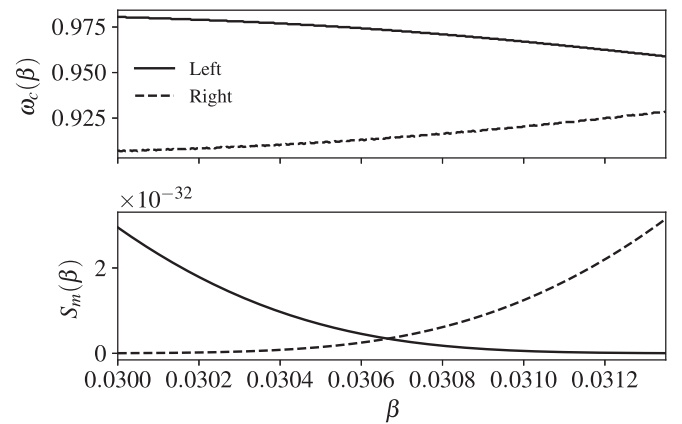


FIG. 4. This figure shows that the left and right modes that are created in the scattering process are red- and blueshifted as the dimensionless parameter β increases. The upper part shows the dimensionless center frequency of each mode as a function of β (in normalized units as well). This is the non-Hermitian correlation-induced spectral shift. The bottom part shows the peak value of the dimensionless spectral density of each mode as β varies. At the intersection of these two curves (around $\beta \approx 0.0306$), the switching of the maxima occurs.

β . The center frequency of the left mode is redshifted, while the center frequency of the right mode is blueshifted as β increases. This synchronized double shift effect is absent in the Hermitian formulation of the scattering problem. It only happens when the material has gain and loss. The bottom part of Fig. 4 shows the peak value of the left and right mode as a function of β . Since they switch locations, the intersection of the two curves gives us the critical value β_c at which the discontinuity of ω_c occurs. One might wonder why we did not just differentiate Eq. (13) with respect to ω , equate it to zero, and calculate the critical points in this way. This is a perfectly valid procedure. However, the obtained expressions are not particularly illuminating (it generates a third-degree polynomial whose expressions for the roots are very complicated) and many of the most important aspects of the spectrum can be obtained by the simpler analysis that we explain later. We will demonstrate in a moment that ω_c depends on the size of the material as well on the scattering angle and this offers a possibility to control the scattered spectrum. It should be pointed out that analogous spectral anomalies have been noticed in diffraction-based systems [37–42]. Our results indicate that the asymmetrical splitting effect can also be tuned by controlling the non-Hermitian properties of the material in scattering-based systems. Also, we provide analytical formulas to characterize this tuning in a more efficient fashion.

Every non-Hermitian aspect involved in the scattering process can be understood by inspecting the polynomial $p_\beta(\omega)$ since this is the only quantity in the spectral density that depends on β . We now demonstrate how the splitting of the Hermitian spectrum into two asymmetrical modes occurs as β increases. First, since we are borrowing the same numerical parameters from [11], the width of the Gaussian profile $h(\omega)$ centered at 0 is $\Gamma_1 = 0.0076$, which is much smaller than the center frequency of $g(\omega)$. This implies that in the product $g(\omega)h(\omega)p_\beta(\omega)$, the effect of $h(\omega)$ is essentially a multiplication by an approximately constant value *in the range of frequencies considered below*, which is $\omega \in [0.9, 1.1]$. Let us consider first the Hermitian situation where $\beta = 0$ to understand why there is no splitting inside the spectrum. In this case, $p_0(\omega) = \omega^4$, i.e., a fourth-degree polynomial that has zero as a root with multiplicity four. In the frequency range of interest, the product between the Gaussian $g(\omega)$ and the polynomial $p_0(\omega) = \omega^4$ will result in a distortion of the Gaussian profile centered at 1. This is the origin of the correlation-induced spectral shifts present in Hermitian scattering scenarios [8]. The center frequency at which the spectral density is a maximum also changes because the critical points of a Gaussian function get modified if you multiply it by a polynomial. So, there is a shift on the maximum value taken by $S_{\beta=0}$, but there is no splitting. On the other hand, if we activate the loss and gain properties of the material, $\beta \neq 0$, then the polynomial $p_\beta(\omega)$ has new root dynamics. Figure 5 shows the resultant effect of multiplying the polynomial $p_\beta(\omega)$ by the function $g(\omega)$ as β varies. It can be seen from this figure that there is a unique root of $p_\beta(\omega)$ that penetrates the region inside the spectrum, causing the aforementioned splitting. The blue line in Fig. 5 represents $p_\beta(\omega)$, the orange line represents the Gaussian $g(\omega)$, and the dashed line represents the resultant spectrum [taking into

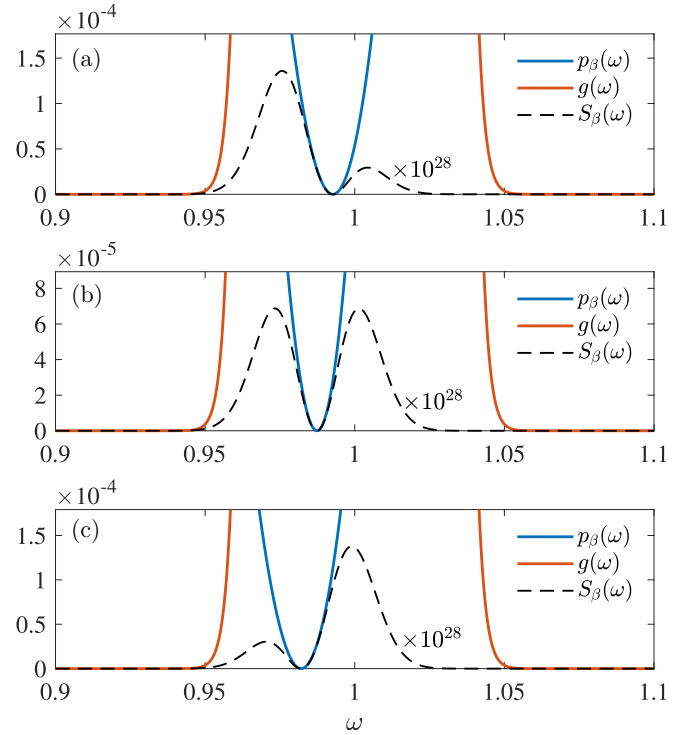


FIG. 5. This figure shows how the form of Eq. (13) allows the creation of two modes inside the bandwidth of the scattered radiation as the dimensionless non-Hermitian parameter β varies. The orange curves represent the (dimensionless) Gaussian function centered at 1, the dashed lines represent the resultant (dimensionless) spectrum $S_\beta(\omega)$, and the blue lines represent the (dimensionless) polynomial $p_\beta(\omega)$ for (a) $\beta = 0.030500$, (b) $\beta = 0.030665$, and (c) $\beta = 0.030830$. The root of the polynomial swaps the frequency band as β varies and this induces the mode creation. The plot of the Gaussian function centered at $\omega = 0$ is not shown here since it has approximately a constant value inside the frequency range that is considered.

account the function $h(\omega)$, which contributes with an overall multiplicative constant in this domain]. The nontrivial root of the polynomial $p_\beta(\omega)$ is easily found from Eq. (13),

$$\omega_r = \frac{1}{2\sigma^2\beta \sin^2(\theta/2)}. \quad (18)$$

It is important to mention that the non-Hermitian spectrum shown in Fig. 3 is about three orders of magnitude smaller than the Hermitian case. To see why this is so, we rewrite Eq. (16) using Eq. (18):

$$p_\beta(\omega) = \omega^4 \left(1 - \frac{\omega}{\omega_r}\right)^2. \quad (19)$$

So, as long as the frequency distribution is close to the root of $p_\beta(\omega)$, i.e., $\omega/\omega_r \approx 1$, this implies that $p_\beta(\omega) < p_0(\omega)$. Therefore, the magnitude of the split spectra will be smaller than the Hermitian case.

Since the polynomial, and therefore its roots, depends on the non-Hermitian parameter β , Eq. (18) can be used to control the splitting of the spectrum in a predetermined manner. For example, regarding Fig. 5 where $\sigma = 6\pi$ and $\theta = 24.9^\circ$, Eq. (18) gives $\omega_r \approx \frac{1}{33\beta}$, and then one can choose the value

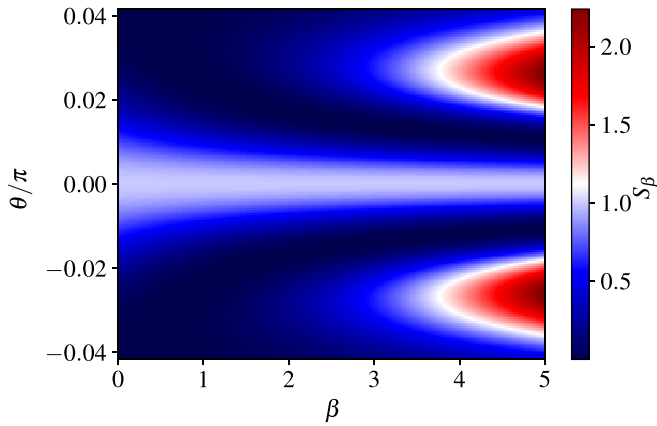


FIG. 6. Spectral density of the scattered radiation field for a fixed frequency $\omega = 1$, where S_β , ω , and β are dimensionless. The red-shaded areas indicate new scattering angles that are forbidden in the Hermitian configuration.

of β such that the root ω_r falls inside the spectrum being split. Alternatively, one can fix the non-Hermitian parameter β along with the scattering direction θ and determine the size of the material (by changing σ) such that a splitting occurs. This manipulation could be used to exclude a very specific frequency inside the original Hermitian scattered spectrum since the root of the polynomial implies that $S_\omega(\omega)$ is exactly zero at the critical point. Clearly, the polynomial p_β contains all the significant characteristics necessary for a practical description of the scattering process.

B. Space analysis

Let us turn now to the directional properties of the scattered radiation. If we fix $\omega = 1$, then the spectral density (13) can be viewed as a function of θ . We are again interested in which directions receive most of the scattered radiation and which receive less. In the Hermitian case, the maximum value of $S_0(\theta)$ is at $\theta = 0$, meaning that a strong part of the scattered field is in the same direction as the incident wave, a well-known result. Figure 6 illustrates the general behavior when $\beta \neq 0$. It is seen that the material's gain and loss properties induce new scattering directions that are originally forbidden in the Hermitian configuration. The new range of scattering angles is depicted by the red-shaded area indicated in the two-dimensional map of Fig. 6. Quantitatively, we are interested in the critical points for which the spectral density is a maximum or a minimum. It is easy to see that the critical points θ_j

$[dS_\beta(\theta_j)/d\theta = 0]$ are solutions of the algebraic equation

$$\sin \theta_j \left(1 - 2\beta\sigma^2 \sin^2 \frac{\theta_j}{2} \right) \left(1 + \beta - 2\beta\sigma^2 \sin^2 \frac{\theta_j}{2} \right) = 0. \quad (20)$$

In the Hermitian case, Eq. (20) turns into $\sin \theta_j = 0$, which gives $\theta_1 = 0$ and $\theta_2 = \pi$, as discussed above. In the non-Hermitian situation ($\beta \neq 0$), these two solutions are still critical points since they both satisfy Eq. (20). However, in this case, four additional solutions are possible:

$$\theta_{3\pm} = \pm 2 \sin^{-1} \left(\frac{1}{\sqrt{2\sigma^2\beta}} \right) \quad (21)$$

and

$$\theta_{4\pm} = \pm 2 \sin^{-1} \left[\sqrt{\frac{1}{2\sigma^2} \left(1 + \frac{1}{\beta} \right)} \right]. \quad (22)$$

These symmetric angles' solutions can be viewed in Fig. 6. A more detailed analysis (not shown) reveals that $\theta_{3\pm}$ ($\theta_{4\pm}$) is a minimum (maximum) of $S_\beta(\theta)$. For the parameters used in Fig. 6, $\sigma = 6\pi$, and taking, for example, $\beta = 4$, the spectral density has the critical points

$$\begin{aligned} \theta_{3\pm}/\pi &= \pm 0.0119 \text{ (minimum),} \\ \theta_{4\pm}/\pi &= \pm 0.0267 \text{ (maximum),} \end{aligned} \quad (23)$$

which can be checked by inspecting Fig. 6. Relations (21) and (22) can be used to select a desired scattering angle simply by adjusting the loss and gain properties of the material. The new scattering directions are not influenced by the material's geometry (σ is maintained fixed) but depend solely on the gain and loss properties of the scatterer.

V. CONCLUSIONS

The spectral density of stochastic scattered radiation by non-Hermitian materials is calculated analytically and its properties are discussed. We have found that the spectrum of scattered radiation is strongly influenced by the gain and loss properties of the material in such a way that it can split the original Hermitian spectrum into two asymmetrical bands. We show how to use the information present in the spectral density to tune the scattered spectrum into a desired pattern as well as the directional properties of the radiation in real space.

ACKNOWLEDGMENT

The authors would like to acknowledge the Brazilian Agency CAPES for financial support.

- [1] E. Wolf and L. Mandel, *Optical Coherence and Quantum Optics* (Cambridge University Press, Cambridge, 1995).
- [2] J. W. Goodman, *Statistical Optics* (Wiley, New York, 2015).
- [3] E. Wolf, *Introduction to the Theory of Coherence and Polarization of Light* (Cambridge University Press, Cambridge, 2007).
- [4] M. J. Beran and G. B. Parrent, *Theory of Partial Coherence* (Prentice-Hall, New Jersey, 1964).

- [5] E. Wolf, Invariance of the Spectrum of Light on Propagation, *Phys. Rev. Lett.* **56**, 1370 (1986).
- [6] E. Wolf, Non-cosmological redshifts of spectral lines, *Nature (London)* **326**, 363 (1987).
- [7] F. Gori, G. Guattari, C. Palma, and C. Padovani, Observation of optical redshifts and blueshifts produced by source correlations, *Opt. Commun.* **67**, 1 (1988).

- [8] E. Wolf and D. F. V. James, Correlation-induced spectral changes, *Rep. Prog. Phys.* **59**, 771 (1996).
- [9] E. Wolf, J. T. Foley, and F. Gori, Frequency shifts of spectral lines produced by scattering from spatially random media, *J. Opt. Soc. Am. A* **6**, 1142 (1989).
- [10] A. Dogariu and E. Wolf, Spectral changes produced by static scattering on a system of particles, *Opt. Lett.* **23**, 1340 (1998).
- [11] M. Lahiri and E. Wolf, Spectral changes of stochastic beams scattered on a deterministic medium, *Opt. Lett.* **37**, 2517 (2012).
- [12] T. Wang and D. Zhao, Effects of source correlation on the spectral shift of light waves on scattering, *Opt. Lett.* **38**, 1545 (2013).
- [13] C. E. Rüter, K. G. Makris, R. El-Ganainy, D. N. Christodoulides, M. Segev, and D. Kip, Observation of parity-time symmetry in optics, *Nat. Phys.* **6**, 192 (2010).
- [14] A. Zyablovsky, A. P. Vinogradov, A. A. Pukhov, A. V. Dorofeenko, and A. A. Lisyansky, \mathcal{PT} -symmetry in optics, *Phys. Usp.* **57**, 1063 (2014).
- [15] S. Longhi, Parity-time symmetry meets photonics: A new twist in non-Hermitian optics, *Europhys. Lett.* **120**, 64001 (2018).
- [16] C. M. Bender and S. Boettcher, Real Spectra in Non-Hermitian Hamiltonians Having \mathcal{PT} symmetry, *Phys. Rev. Lett.* **80**, 5243 (1998).
- [17] C. M. Bender, S. Boettcher, and P. N. Meisinger, \mathcal{PT} -symmetric quantum mechanics, *J. Math. Phys.* **40**, 2201 (1999).
- [18] C. M. Bender, Making sense of non-Hermitian Hamiltonians, *Rep. Prog. Phys.* **70**, 947 (2007).
- [19] C. M. Bender, D. C. Brody, and H. F. Jones, Must a Hamiltonian be Hermitian? *Am. J. Phys.* **71**, 1095 (2003).
- [20] C. M. Bender, Introduction to \mathcal{PT} -symmetric quantum theory, *Contemp. Phys.* **46**, 277 (2005).
- [21] C. M. Bender, D. C. Brody, and H. F. Jones, Complex Extension of Quantum Mechanics, *Phys. Rev. Lett.* **89**, 270401 (2002).
- [22] A. Mostafazadeh, Pseudo-Hermiticity versus \mathcal{PT} symmetry: The necessary condition for the reality of the spectrum of a non-Hermitian Hamiltonian, *J. Math. Phys.* **43**, 205 (2002).
- [23] A. Mostafazadeh, Pseudo-Hermiticity versus \mathcal{PT} -symmetry. II: A complete characterization of non-Hermitian Hamiltonians with a real spectrum, *J. Math. Phys.* **43**, 2814 (2002).
- [24] A. Mostafazadeh, Pseudo-Hermiticity versus \mathcal{PT} -symmetry III: Equivalence of pseudo-Hermiticity and the presence of antilinear symmetries, *J. Math. Phys.* **43**, 3944 (2002).
- [25] W. Heiss, The physics of exceptional points, *J. Phys. A: Math. Theor.* **45**, 444016 (2012).
- [26] Z. Lin, H. Ramezani, T. Eichelkraut, T. Kottos, H. Cao, and D. N. Christodoulides, Unidirectional Invisibility Induced by \mathcal{PT} -Symmetric Periodic Structures, *Phys. Rev. Lett.* **106**, 213901 (2011).
- [27] M. Liertzer, L. Ge, A. Cerjan, A. D. Stone, H. E. Türeci, and S. Rotter, Pump-Induced Exceptional Points in Lasers, *Phys. Rev. Lett.* **108**, 173901 (2012).
- [28] H. Hodaei, M.-A. Miri, M. Heinrich, D. N. Christodoulides, and M. Khajavikhan, Parity-time-symmetric microring lasers, *Science* **346**, 975 (2014).
- [29] T. Wasak, P. Szańkowski, V. V. Konotop, and M. Trippenbach, Four-wave mixing in a parity-time (\mathcal{PT})-symmetric coupler, *Opt. Lett.* **40**, 5291 (2015).
- [30] S. Weimann, M. Kremer, Y. Plotnik, Y. Lumer, S. Nolte, K. G. Makris, M. Segev, M. C. Rechtsman, and A. Szameit, Topologically protected bound states in photonic parity-time-symmetric crystals, *Nat. Mater.* **16**, 433 (2017).
- [31] P. A. Brandão and S. Cavalcanti, Non-Hermitian spectral changes in the scattering of partially coherent radiation by periodic structures, *Opt. Lett.* **44**, 4363 (2019).
- [32] P. A. Brandão and S. B. Cavalcanti, Scattering of partially coherent radiation by non-Hermitian localized structures having parity-time symmetry, *Phys. Rev. A* **100**, 043822 (2019).
- [33] J. Jansson, T. Jansson, and E. Wolf, Spatial coherence discrimination in scattering, *Opt. Lett.* **13**, 1060 (1988).
- [34] D. F. James and E. Wolf, Doppler-like frequency shifts generated by dynamic scattering, *Phys. Lett. A* **146**, 167 (1990).
- [35] E. Wolf and J. T. Foley, Scattering of electromagnetic fields of any state of coherence from space-time fluctuations, *Phys. Rev. A* **40**, 579 (1989).
- [36] E. Wolf, Diffraction of radiation of any state of spatial coherence on media with periodic structure, *Opt. Lett.* **38**, 4023 (2013).
- [37] J. Pu and S. Nemoto, Spectral shifts and spectral switches in diffraction of partially coherent light by a circular aperture, *IEEE J. Quantum Electron.* **36**, 1407 (2000).
- [38] G. Gbur, T. D. Visser, and E. Wolf, Anomalous Behavior of Spectra Near Phase Singularities of Focused Waves, *Phys. Rev. Lett.* **88**, 013901 (2001).
- [39] G. Popescu and A. Dogariu, Spectral Anomalies at Wave-Front Dislocations, *Phys. Rev. Lett.* **88**, 183902 (2002).
- [40] S. A. Ponomarenko and E. Wolf, Spectral anomalies in a Fraunhofer diffraction pattern, *Opt. Lett.* **27**, 1211 (2002).
- [41] T. Visser and E. Wolf, Spectral anomalies near phase singularities in partially coherent focused wave fields, *J. Opt. A: Pure Appl. Opt.* **5**, 371 (2003).
- [42] J. Pu, C. Cai, and S. Nemoto, Spectral anomalies in Young's double-slit interference experiment, *Opt. Express* **12**, 5131 (2004).